

A high energy photon polarimeter for astrophysics

Maxim Eingorn, Lakma Fernando, Branislav Vlahovic¹

North Carolina Central University, 1801 Fayetteville St., Durham, NC 27707, USA

Cosmin Ilie

University of North Carolina, Chapel Hill, NC 27599, USA

Bogdan Wojtsekhowski²

Thomas Jefferson National Accelerator Facility, Newport News, VA 23606, USA

Guido Maria Urciuoli, Fulvio De Persio

INFN, Sezione di Roma, I-00185 Rome, Italy

Franco Meddi

INFN, Sezione di Roma and Sapienza Università di Roma, I-00185 Rome, Italy

ABSTRACT

A high-energy photon polarimeter for astrophysics studies in the energy range from 20 MeV to 1000 MeV is considered. The proposed concept uses a stack of silicon micro-strip detectors where they play the roles of both a converter and a tracker. The purpose of this paper is to outline the parameters of such a polarimeter and to estimate the productivity of measurements. Our study supported by a Monte Carlo simulation shows that with a one-year observation period the polarimeter will provide 6% accuracy of the polarization degree for a photon energy of 100 MeV, which would be a significant advance relative to the currently explored energy range of a few MeV. The proposed polarimeter design could easily be adjusted to the specific photon energy range to maximize efficiency if needed.

1. Introduction

Recent discoveries have underlined a key role of astrophysics in the study of nature. In this paper we are presenting a potential instrument for measuring high energy photon polarization with

¹Corresponding author e-mail: vlahovic@nccu.edu

²Corresponding author e-mail: bogdanw@jlab.org

a proven detector technique which should allow preparation of a reliable tool for the space-borne observatory.

Polarization of the photon has played an important role (sometimes even before it was recognized) in physics discoveries such as the famous Young’s interference experiment (Young 1802), Michelson-Morley’s test of the Ether theory (Michelson 1887), determination of the neutral pion parity (Yang 1950) and many others, including more recently the spin structure of the nucleon (Aidala 2013). Polarization of the Cosmic Microwave Background (CMB) will likely be a crucial observable for the inflation theory (see PLANCK [sci.esa.int/planck] and BICEP [bicepkeck.org] results).

During the last decade, observations from the AGILE [agile.rm.iasf.cnr.it] and FERMI-LAT [www-glast.stanford.edu] pair production telescopes have enhanced our understanding of gamma (γ) ray astronomy. With the help of these telescopes numerous high energy γ ray sources have been observed. However, the current measurements are insufficient to fully understand the physics mechanism of such γ ray sources as gamma ray bursts (GRBs), active galactic nuclei (AGNs), blazars, pulsars, and supernova remnants (SNRs). Even though both telescopes cover a wide range of energy (from 20 MeV to more than 300 GeV), neither of them is capable of polarization measurements.

Medium to high energy photon polarimeters for astrophysics were proposed by the NASA group (Bloser 2006) and recently by the Saclay group (Bernard 2012). Both are considering Ar(Xe)-based gas-filled detectors: the Time Projection Chamber with a micro-well or micromegas section for amplification of ionization. In this paper we evaluate the features of an electron-positron pair polarimeter for the full energy range from 20 MeV to 1000 MeV and then propose a specific design for a polarimeter in the 100 to 300 MeV energy range using silicon micro-strip detectors, MSDs, whose principal advantage with respect to the gas-based TPC is that the spatial and two-track resolution is about five to ten times better.

The paper is organized in the following way: In section 2 we briefly discuss the motivation for cosmic γ ray polarimetry in the high energy region. Section 3 is devoted to measurement techniques, polarimeters being built and current proposals. In section 4 we calculate the photon flux coming from the Crab Pulsar and Crab Nebula. The design of the new polarimeter and its performance are discussed in the last few sections.

2. Scientific Motivation

There are several recent reviews of photon polarimetry in astrophysics (Lei 1997; McConnell 2004, 2006; Krawczynski 2011; Hajdas 2013; Pohl 2014) which address many questions which we just briefly touch on in this section. Photon polarimetry for energy below a few MeV is a very active field of astrophysical research, and some examples of the productive use of polarimetry at these energies include: detection of exoplanets, analysis of chemical composition of planetary atmosphere, and investigation of interstellar matter, quasar jets and solar flares. However, no

polarization measurements are available in the medium and high energy regions because of the instrumental challenges.

The primary motivation in proposing a polarimeter is our interest in understanding the emission and production mechanisms for polarized γ rays in pulsars, GRBs, and AGNs by measuring polarization of cosmic γ rays in this under-explored energy region ($\sim 100 - 1000$ MeV). Additionally, the polarization observations from the rotation-powered and accretion-powered pulsar radiation mechanisms could help to confirm the identification of black hole candidates (Dovciak 2008).

Polarization measurements could reveal one of the possible effects induced by quantum gravity, the presence of small, but potentially detectable, Lorentz or CPT violating terms in the effective field theory. These terms lead to a macroscopic birefringence effect of the vacuum (see (Jacobson 2006) for more information). Up to now, the highest energy linear polarization measurement has been for GRB 061122 in the 250-800 keV energy range (Gotz 2013), and vacuum birefringence has not been observed in that region. Therefore, extending polarization sensitivity to higher energies could lead to detection of vacuum birefringence, which would have an extraordinary impact on fundamental physics, or in the case of null detection we could significantly improve the present limits on the Lorentz Invariance Violation parameter.

Further, according to the observations by the Energetic Gamma Ray Experiment Telescope (EGRET) [heasarc.gsfc.nasa.gov/docs/cgro/egret], the synchrotron emission of the Crab Nebula is significant in the energy below ~ 200 MeV (Jager 1996). Additionally, the theoretical studies state that most of the γ rays coming from the Crab Nebula around 100 MeV may come from its inner knot (Komissarov 2011), so the observations in the neighborhood of 100 MeV will help to test this theoretical hypothesis and confirm the emission mechanism. Furthermore, the observation of the γ rays from the Crab Pulsar provides strong evidence of the location of the γ ray emitting region as it lies in the center of the Nebula.

It is also worth mentioning that polarimetry could test the theories assuming existence of axions (hypothetical particles introduced to solve the strong CP problem of QCD). It is interesting that the same axions or axion-like particles can serve as a foundation for a relevant mechanism of Sun luminosity (Rusov 2014). A theoretical study (Rubbia 2008) has shown that polarization observations from GRBs can be used to constrain the axion-photon coupling: $g_{a\gamma\gamma} \leq 2.2 \times 10^{-11} \text{ GeV}^{-1}$ for the axion mass 10^{-3} eV. The limit of the coupling scales is $\propto 1/\sqrt{E}$; therefore, the polarimetry of GRBs at higher energies would lead to tighter constraints.

In two of the following subsections we will briefly explain how polarization measurements are involved in confirming the emission mechanism and geometry of two above-mentioned sources.

2.1. Pulsars

Pulsars are a type of neutron star, yet they are highly magnetized and rotate at enormous speeds. The questions concerning the way magnetic and electric fields are oriented, how particles are accelerated and how the energy is converted into radio and γ rays in pulsars are still not fully answered. Because of the extreme conditions in pulsars' interiors, they can be used to understand poorly known properties of superdense, strongly magnetized, and superconducting matter (Guo 2014; Buballa 2014). Moreover, by studying pulsars one can learn about the nuclear reactions and interactions between the elementary particles under these conditions, which cannot be reproduced in terrestrial laboratories. Particle acceleration in the polar region of the magnetic field results in gamma radiation, which is expected to have a high degree of polarization (Kaspi 2004). Depending on the place where the radiation occurs, the pulsar emission can be explained in the framework of a polar cap model or an outer cap model. In both models, the emission mechanism is similar, but polarization is expected to be dissimilar (McConnell 2009); hence, polarimetry could be used to understand the pulsar's emission mechanism.

2.2. Gamma Ray Bursts

Polarization measurements would also help to understand GRBs. The GRBs (Meszaros 2006) are short and extremely bright bursts of γ rays. Usually, a short-time (from 10^{-3} s to about 10^3 s) peak of radiation is followed by a long lasting afterglow. The characteristics of the radiation emitted during the short-time peak and during the afterglow are different. The number of high-energy photons which may be detected during the short-time burst phase is expected to be small compared with the one for the long-lived emission. While only about 3% of the energy emitted during the short-time burst is carried by high-energy photons with $E > 100$ MeV, the high energy photons of the afterglow carry about half of the total emitted energy. Therefore, there is a possibility of observing polarization of high energy photons during the afterglow. The emission mechanism of GRBs, the magnetic composition, and the geometry and morphology of GRB jets are still uncertain but can be at least partly revealed in this way.

It is worth noting that several studies have discussed how the degree of polarization, P , depends on the GRB emission mechanisms. In one example, using Monte Carlo methods Toma *et al.* (Toma 2009) showed that the Compton drag model is favored when the degree of polarization $P > 80\%$, and $P \sim 20\%-70\%$ concerns the synchrotron radiation with the ordered magnetic fields model. Moreover, studies by Mundell *et al.* (Mundell 2013) and Lyutikov *et al.* (Lyutikov 2003) have proven that polarimetry could assist in revealing the geometry of GRB jets.

3. Photon Polarimetry in Astrophysics Research

Several physical processes such as the photoelectric effect, Thomson scattering, Compton scattering, and electron-positron pair production can be used to measure photon linear polarization. Polarimeters based on the photoelectric effect and Thomson scattering are used at very low energies. Compton polarimeters are commonly used for energies from 50 keV to a few MeV (Lei 1997; McConnell 2004, 2006; Krawczynski 2011; Hajdas 2013; Pohl 2014).³

Some of the major achievements in astrophysics that were obtained using polarimetry are: the discovery of synchrotron radiation from the Crab Nebula (Oort 1956); the study of the surface composition of solar system objects (Bowell 1974); the measurement of the X-ray linear polarization of the Crab Nebula (Weisskopf 1978), which is still one of the best measurements of linear polarization for astrophysical sources; mapping of solar and stellar magnetic fields (Schrijver 2000); detection of polarization in the CMB radiation (Kovac 2002); and analysis of large scale galactic magnetic fields (Kulsrud 2008).

The measurement of polarization in this high energy γ ray regime can be done by detecting the electron-positron pairs produced by γ rays and analysis of a non-uniformity of event distribution in the electron-positron pair plane angle, as discussed in Ref. (Kelner 1975). However, implementation of this technique should consider limitations due to multiple Coulomb scatterings in the detector, and there are no successful polarization measurements for astrophysical sources in the energy regime of interest in our paper.

A number of missions have included cosmic γ ray observations, but only a few of them are capable of measuring polarization. The polarimetry measurements were mainly restricted to γ rays with low energies $E < 10$ MeV. As an example, the Reuven Ramaty High Energy Solar Spectroscopic Imager (RHESSI) [hesperia.gsfc.nasa.gov/rhessi3], launched to image the Sun at energies from 3 keV to 20 MeV, was capable of polarimetry up to 2 MeV, and the results were successfully used to study the polarization of numerous solar flares (McConnell 2003; Boggs 2006).

The SPI detector INTErnational Gamma-Ray Astrophysics Laboratory (INTEGRAL) instrument [sci.esa.int/integral] has the capability of detecting polarization in the range of 3 keV to 8 MeV (Lei 1997; Forot 2007). It was used to measure the polarization of GRB 041219a, and later a high degree of polarization of γ rays from that source (McGlynn 2007; Kalemci 2007) was confirmed. The Tracking and Imaging Gamma Ray Experiment (TIGRE) Compton telescope, which observes γ rays in the range of 0.1 – 100 MeV, can measure polarization up to 2 MeV.

Recently, Morselli *et al.* proposed GAMMA-LIGHT to detect γ rays in the energy range 10 MeV – 10 GeV, and they believe that it will provide solutions to all the current issues that

³Those polarimeters are not efficient at a photon energy of 100 MeV because kinematical suppression of the Compton rate at large scattering angles leads to a fast drop in the analyzing power (as $1/E_\gamma$) above an energy range of a few MeV.

could not be resolved by AGILE and FERMI-LAT in the energy range 10 – 200 MeV. It can also determine the polarization for intense sources for the energies above a few hundred MeV with high accuracy (Morselli 2013).

In spite of the limitations of the instruments’ capability, there are numerous polarimetry studies in γ ray astrophysics, and various proposals have been put forth regarding medium and high energy γ ray polarimeters. For example, Bloser *et al.* (Bloser 2006) proposed the advanced pair telescope (APT), also a polarimeter, in the ~ 50 MeV – 1 GeV range. That proposal uses a gas-based Time Projection Chamber (TPC) with micro-well amplification to track the e^+ , e^- path. The polarization sensitivity was estimated by using Geant4 Monte Carlo simulations. Preliminary results indicated that it will be capable of detecting linearly polarized emissions from bright sources at 100 MeV. As an updated version of the APT, Hunter *et al.* (Hunter 2014) suggested the Advanced Energetic Pair Telescope (AdEPT) for γ ray polarimetry in the medium energy range; further, they mentioned that it would also provide better photon angular resolution than FERMI-LAT in the range of ~ 5 to ~ 200 MeV.

HARPO is a hermetic argon TPC detector proposed by Bernard *et al.* (Bernard 2012) which would have high angular resolution and would be sensitive to polarization of γ rays with energies in the MeV-GeV range. A demonstrator for this TPC was built, and preliminary estimates of the spatial resolution are encouraging. Currently, the HARPO team is finalizing a demonstrator set up to characterize a beam of polarized γ rays in the energy range of 2 – 76 MeV (Bernard 2014).

4. The photon flux from the Crab system

Observations of the γ rays from the Crab Pulsar and Crab Nebula have been reported in Ref. (Abdo 2010) for eight months of survey data with FERMI-LAT. The pulsar dominates the phase-averaged photon flux, but there is an off-pulse window (35% of the total duration of the cycle) when the pulsar flux is negligible and it is therefore possible to observe the nebular emission. According to the conducted analysis, the spectrum of the Crab Nebula in the 100-300 MeV range can be described by the following combined expression:

$$\frac{dN}{dE} = N_{\text{sync}} E^{-\Gamma_{\text{sync}}} + N_{\text{IC}} E^{-\Gamma_{\text{IC}}}, \quad (1)$$

where the quantity dN/dE is measured in $\text{cm}^{-2}\text{s}^{-1}\text{MeV}^{-1}$ representing the number of photons reaching 1 cm^2 of the detector area per second, per 1 MeV of energy. The energy E on the right hand side is measured in GeV. The prefactors $N_{\text{sync}} \approx 9.1 \times 10^{-13} \text{ cm}^{-2}\text{s}^{-1}\text{MeV}^{-1}$ and $N_{\text{IC}} \approx 6.4 \times 10^{-12} \text{ cm}^{-2}\text{s}^{-1}\text{MeV}^{-1}$ are determined by 35% of the total duration of the cycle, while $\Gamma_{\text{sync}} \approx 4$ and $\Gamma_{\text{IC}} \approx 1.65$. The first and second terms on the right hand side, as well as the indices "sync" and "IC", correspond to the synchrotron and inverse Compton components of the spectrum, respectively. As one can see, these terms have different dependence on the energy E since they represent different contributions to the total spectrum. The first part (the synchrotron radiation)

comes from emission by high energy electrons in the nebular magnetic field while the second part is due to the inverse Compton scattering of the primary accelerated electrons.

For convenience let us rewrite the expression for the spectrum of the Crab Nebula in the form

$$\frac{dN}{dE} = \tilde{N}_{\text{sync}} E^{-\Gamma_{\text{sync}}} + \tilde{N}_{\text{IC}} E^{-\Gamma_{\text{IC}}}, \quad (2)$$

where the energy E on both sides is now measured in MeV, so $\tilde{N}_{\text{sync}} \approx 9.1 \times 10^{-1} \text{ cm}^{-2} \text{ s}^{-1} \text{ MeV}^{-1}$ and $\tilde{N}_{\text{IC}} \approx 5.7 \times 10^{-7} \text{ cm}^{-2} \text{ s}^{-1} \text{ MeV}^{-1}$. Integrating dN/dE , for the photon flux above 100 MeV coming from the Crab Nebula we obtain the number $\sim 3.5 \times 10^{-7} \text{ cm}^{-2} \text{ s}^{-1}$ giving for the total cycle duration $\sim 10^{-6} \text{ cm}^{-2} \text{ s}^{-1}$, or $\sim 3 \times 10^5 \text{ m}^{-2} \text{ y}^{-1}$.

At the same time the averaged spectrum of the Crab Pulsar is described in (Abdo 2010) as follows:

$$\frac{dN}{dE} = N_0 E^{-\Gamma} \exp\left(-\frac{E}{E_c}\right), \quad (3)$$

where $N_0 \approx 2.36 \times 10^{-4} \text{ cm}^{-2} \text{ s}^{-1} \text{ MeV}^{-1}$, $\Gamma \approx 2$ and the cut-off energy $E_c \approx 5800 \text{ MeV}$. As before, the energy E on both sides is measured in MeV. Integrating this expression, for the photon flux above 100 MeV coming from the Crab Pulsar we obtain the number $\sim 2 \times 10^{-6} \text{ cm}^{-2} \text{ s}^{-1}$, or $\sim 6 \times 10^5 \text{ m}^{-2} \text{ y}^{-1}$. Thus, the Pulsar's photon flux is twice as intensive as the Nebula's. A fast photometer could be insert in the polarimeter instrumentation to collect events and have a temporal tag and consequently distinguish between nebula and pulsar photons, see e.g. (Meddi 2012).

We will use the numbers above for an estimation of the polarimeter results at a 100 MeV energy cut. For a 500 MeV cut the statistics drops by a factor of five (because E_c is much higher the exponential factor does not play a role) .

It is worth noting that the estimates following from (Abdo 2010) approximately agree with the corresponding estimates made in (Buehler 2012) (where the formulas (1) and (2) describe the synchrotron and inverse Compton components of the Crab Nebula spectrum while the formula (3) describes the averaged Crab Pulsar spectrum). Really, according to (Buehler 2012), the total Crab Nebula photon flux above 100 MeV is $\sim 7.2 \times 10^{-7} \text{ cm}^{-2} \text{ s}^{-1}$, while for the Crab Pulsar the value again reads $\sim 2 \times 10^{-6} \text{ cm}^{-2} \text{ s}^{-1}$.

5. The photon polarimetry with pair production

The photo production of an electron-positron pair in the field of nuclei is a well understood process which was calculated in QED with all details including the effect of photon linear polarization, see e.g. Ref. (Maximon 1959). The kinematics and variables of the reactions are shown in Fig. 1. The distribution of events over an azimuthal angle $\phi_{+(-)}$ of a positron (electron) relative to the direction of an incident photon has the following form:

$dN/d\phi_{\pm} \propto 1 + A \cdot P_{\gamma} \cdot \cos 2(\phi_{+(-)} + \Delta)$, where A is the analyzing power, P_{γ} is the degree of the photon linear polarization, and Δ is the angle of the photon linear polarization vector in the detector coordinate system. In practice (Bogdan 2003), angle ω_{\pm} could be used instead of $\phi_{+(-)}$ because at the photon energies of interest the co-planarity angle $\phi_{\pm} \sim 180^{\circ}$.

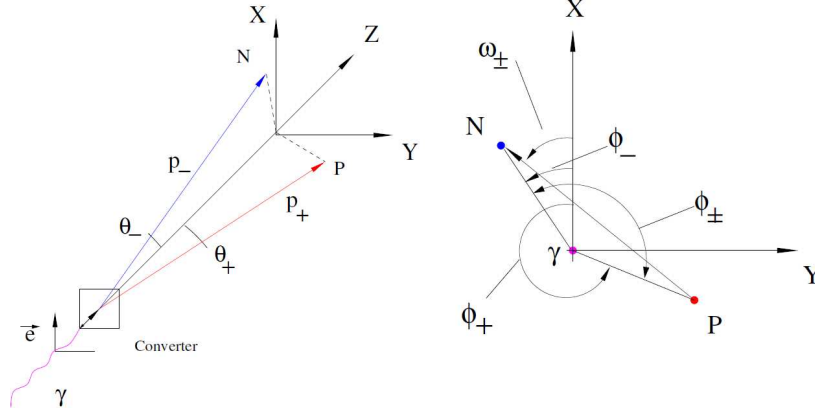


Fig. 1.— The kinematics of e^+e^- pair photo production (left picture) and the azimuthal angles in the detector plane from Ref. (Bogdan 2003). The photon momentum is directed along the Z axis. The photon polarization vector \vec{e} is parallel to the X axis. The angle ϕ_+, ϕ_- is the angle between the photon polarization plane and the plane constructed by the momentum of the photon and the momentum of the positron (the electron). The angle ϕ_{\pm} is called the co-planarity angle. The labels P and N indicate the positions of the crossings of the detector plane by the positron and the electron. The azimuthal angle ω_{\pm} between the polarization plane and the vector \overline{PN} is a directly measurable parameter.

The value of analyzing power A was found to be a complicated function of the event parameters and detection arrangement (Maximon 1959). The numerical integration of the full expression could be performed for given conditions, see e.g. (Bogdan 2003). In a high energy limit a compact expression for the integrated analyzing power for the pair photo-production from atomic electron was obtained in Ref. (Boldyshev 1971).

The practical design and the test of the polarimeter for a beam of high energy photons were reported in Ref. (Jager 2004). There we detected both particles of the pair and reconstructed the azimuthal angle of the pair plane ω_{\pm} (see Fig. 1). The analyzing power, averaged over energy sharing between electron and positron and pair open angle of the experimental acceptance, has been found to be 0.116 ± 0.002 , comparable to a 0.14 value as shown in Fig. 2 reproduced from (Bogdan 2003). When the pair components move through the converter, the azimuthal angle built on pair coordinates and pair vertex becomes blurred due to multiple scattering.

It is useful to note that the purpose of development in Ref. (Jager 2004) was a polarimeter for an intense photon beam. The thickness of the converter in the beam polarimeter was chosen

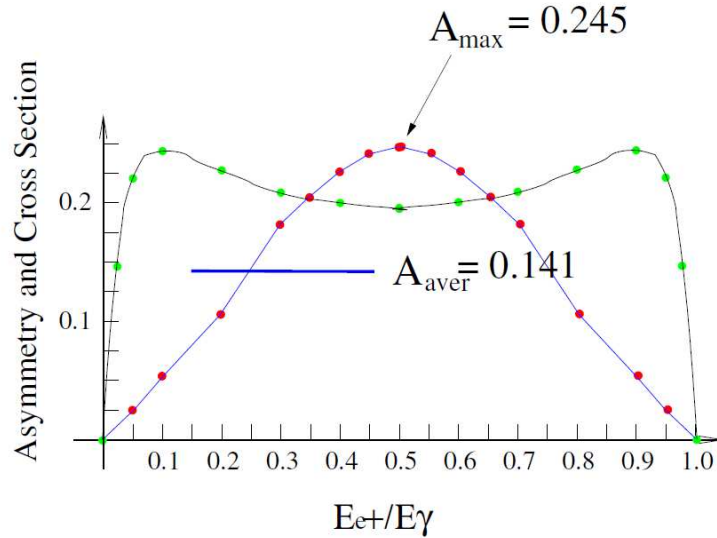


Fig. 2.— The asymmetry (red dots) and cross section (green dots) of pair production by 2 GeV 100% linearly polarized photons as a function of positron energy (Bogdan 2003). A_{aver} shows the asymmetry averaged over the full range of the positron energy.

to be very small to minimize systematics of the measurement of the photon polarization degree. However, the polarimeter could be calibrated by using the highly polarized photon beams produced in the laser-backscattering facilities. For the cosmic ray polarimeter, we propose a larger converter thickness and calibration of the device. Such an approach is more productive for cosmic rays studies where a relative systematic error on the polarization degree at the level of 3-5% is acceptable.

Let us also note that for the photon beam polarimetry there are additional options such as a coherent pair production in an oriented crystal and a magnetic separation of the pair components used many years ago in nuclear physics experiments. For the space-borne photon investigation, those polarimeters are not applicable for the obvious reasons of the limited angle range for the coherent effects and the large weight and power consumption of the magnetic system.

An active converter with a coordinate resolution of a few microns would allow us to construct a dream device, a very efficient polarimeter. A real world active-converter device, a gas-filled TPC, has a spatial resolution of 100 μm and much larger two-track resolution of 1.5-2 mm (for a few cm long drift distance). Such a polarimeter will be a very productive instrument for the photon energy range below 50 MeV. However, because of these resolutions, it would be hard to measure the degree of polarization of photons whose energy is bigger than 100 MeV.

A polarimeter with separation of the converter and pair detector functions could benefit from the high coordinate resolution of the silicon MSD of 10-15 μm , its two-track resolution of 0.2 mm, and flexibility for the distance between a converter and pair hits detector: Between them would be

a vacuum gap.

6. A polarimeter for cosmic γ rays

The key parameters of the polarimeter are the efficiency, ϵ , and analyzing power, A . Here we outline the analysis of the Figure-of-Merit, $FOM = \epsilon \times A^2$. We will consider a polarimeter as a stack of individual flat cells, each of which is comprised of a converter with a two-dimensional coordinate readout and a coordinate detector for two-track events with no material between them.

The thickness of the converter, where the photon produces the electron-positron pair, defines in the first approximation the polarimeter efficiency as follows:

$$\epsilon = \eta_{cell} \times \frac{1 - r^n}{1 - r} \quad (4)$$

The efficiency of one cell is $\eta_{cell} = 1 - \exp(-\frac{7}{9} \times t_{conv})$ with t_{conv} is the thickness of the converter in units of radiation length. The r is the reduction of the photon flux due to absorption in a single cell defined as $r = \exp(-\frac{7}{9} \times t_{cell-r})$, where t_{cell-r} is the thickness of the cell in units of radiation length, and $n = L/t_{cell-g}$ is the number of cells in the device of length L and geometrical thickness of the cell t_{cell-g} .

The converter thickness needs to be optimized because above some thickness it does not improve the FOM or the accuracy of the polarimeter result (see the next section). As it is shown in Fig. 2, selection of the symmetric pairs ($E_+ = E_-$) provides an analyzing power $A_{sim} = 0.25$ while the averaged over pair energy sharing $A_{aver} = 0.14$. However, the value of the FOM is largest when the cut on pair energy sharing is relaxed. The practical case for the energy cut is $E_+, E_- > E_\gamma/4$, which allows us to avoid events with a low value of A and most δ -electron contamination. The average value of A for such a range of $e^+ - e^-$ energy sharing is 0.20.

The energy of the particles and the shower coordinates could be measured by a segmented electromagnetic calorimeter or estimated from the width of the track, which due to multiple scattering is inversely proportional to the particle momentum. In the photon energy range of interest, both electron and positron will pass through a large number of cells. Determination of particle energy based on multiple scattering would provide $\sim 20\%$ relative energy resolution, which is sufficient for the proposed cut $E_+, E_- > E_\gamma/4$. Estimation of the particle energy could also be useful for rejection of the hits in MSDs induced by the δ -electrons.

7. Monte Carlo simulation

A Monte Carlo simulation was used to evaluate the general effects of pair production in the converter and the specific design of the polarimeter.

7.1. Study of the converter thickness effects

We used a Geant3-based MC code to study the photon detection efficiency and electron-positron pair azimuthal distribution in a wide range of the converter thickness up to 10% of radiation length. Because both the pair opening angle and multiple scattering are scaled with the photon energy, the distributions are almost energy independent. We present first the results for the 100 MeV photon energy for different thicknesses of the converter at a fixed distance of 20 mm between the converter end and the detector.

We used a standard Geant3 pair production generator for the unpolarized photons and at the conversion point introduced a weighting factor for each event as $W(\omega_{\pm}) = 1 + A \times \cos 2\omega_{\pm}$ to simulate a polarization effect on an event-by-event basis. The value of azimuthal angle modulation at the pair production point was fixed at 0.20, which is the average value of the analyzing power A at production over the selected range of particle energies. The pair component propagation was realized in the MC, and the track parameters were evaluated.

Fig. 3 shows the summary of MC results. The apparent optimum converter thickness is close to 1 mm for which the projected $A = 0.10$ is reasonably large and the FOM is close to the saturation limit. However, we are expecting that when δ -electron hits are included in analysis the optimum thickness for the 100 MeV photon case will be smaller and the FOM would be a bit lower.

7.2. Detector parameters

The coordinate detector allows determination of the opening angle between the pair components and the azimuthal angle of the pair plane relative to the lab coordinate system, the main variable for measurement of the photon polarization. Such a detector is characterized by the coordinate resolution, σ_x , and the minimum two-track distance, $a_{x,min}$, at which coordinates of two tracks could be determined with quoted σ_x accuracy. The $a_{x,min}$ is typically 2 mm for drift chamber. For TPC with micromega amplification stage and strip-type readout, $a_{x,min}$ is about 4 strips or 1.6 mm (pitch equal to 400 μm). For silicon MSD $a_{x,min}$ is about 0.20 mm (pitch equal to 50 μm).

The opening angle between the pair components is on the order of $4/(E_{\gamma}/m_e)$, where E_{γ} is the photon energy and m_e is the electron rest mass. The events with an opening angle larger than $3/(E_{\gamma}/m_e)$ but less than $9/(E_{\gamma}/m_e)$ provide most of the analyzing power, as it is shown in Ref. (Bogdan 2003). It is easy to find that the resulting geometrical thickness of the cell is $t_{cell-g} = (a_{x,min} \cdot E_{\gamma})/(3 \cdot m_e)$, whose numerical values are shown in Tab. 1.

For photon energies above 100 MeV, the silicon MSD is a preferable option because of the limit on the apparatus's total length. Indeed, considering a 300 cm total length and an energy of 500 MeV, the number of cells is 5 for the drift chamber option, 6 for the TPC/micromega, and 46 for the MSD option. On another side, the total amount of matter in the polarimeter should be limited to one radiation length or less, because of significant absorption of the incident photons

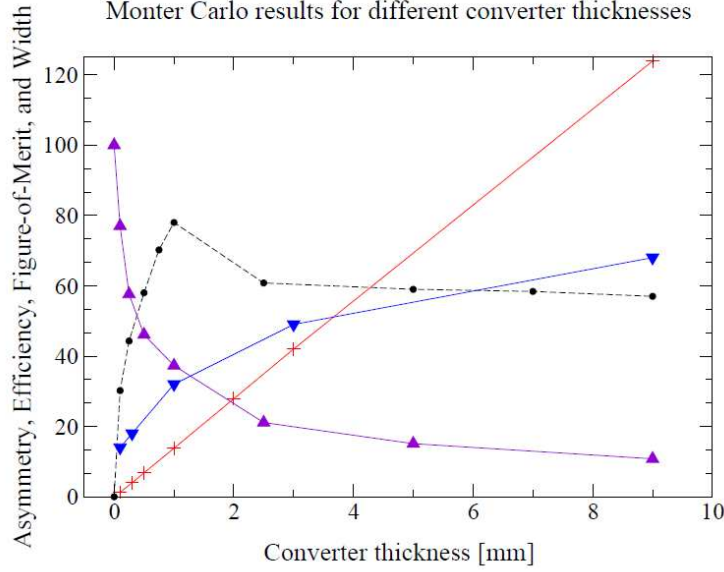


Fig. 3.— Results of MC simulation for 100 MeV photon energy vs. thickness of the converter. The purple set (triangles with the tip toward the bottom) is for the analyzing power (normalized to the value 0.20 at the conversion point). The red set (stars) is the number of e^+e^- pairs with $E_+, E_- > E_\gamma/4$ per 2×10^4 incident photons. The blue set (triangles with the tip toward the top) is for the rms of the difference $\Delta\omega_{\pm}$ between the angle ω_{\pm} at production point and at the detector. The $\Delta\omega_{\pm}$ shows a loss of correlation between production and detection points, in units of 10 mrad. The black set (circles) is the $FOM = \epsilon \times A^2$ in arbitrary units. A cut $r_{+-} > 0.2$ mm was applied on the distance between coordinates of two tracks (for 20 mm between the converter and the detector planes).

which will reduce the average efficiency per cell. For example, in the MSD option 54% absorption will occur with 46 cells (1 mm thickness 2d readout converter detector and two 0.3 mm thickness 1d readout track detectors). The detection efficiency (pair production in the converters) could be estimated as $\epsilon = \eta_{cell} \times \frac{1-r^n}{1-r}$ (Eq. 4), which is about 34% for the selected parameters of the polarimeter. However, the useful statistics result is lower due to a cut on the pair components' energies and contributions of the non-pair production processes, especially at low photon energy. For a photon energy of 100 MeV, the obtained efficiency is 0.28% per cell and the overall efficiency for the 46 cell polarimeter is 9%. The efficiency becomes significantly larger ($\sim 15\%$) for a photon energy of 1000 MeV.

Assuming observation of the Crab pulsar photon source with a 1 m^2 detector for one year the total statistics of pairs (above a 100 MeV photon energy cut) was estimated to be $N_{pairs} = 6 \times 10^5 \times 0.09 = 0.54 \times 10^5$. For the projected analyzing power A of 0.10 the statistical accuracy of

Table 1: The geometrical cell thickness, t_{cell-g} , in **cm** for the different detectors and photon energies.

Photon energy [MeV]	Drift chamber	TPC/micromega	silicon MSD
20	2.6	2	0.26
100	13	10	1.3
500	65	52	6.5
2000	260	210	26

the polarization measurement is $\sigma_P = \frac{1}{A} \times \sqrt{\frac{2}{N_{pairs}}} \approx 0.06$ for the MSD detector option. Realization of such high accuracy would require a prior calibration of the polarimeter at a laser-back scattering facility.

7.3. Geometry of the MSD-based polarimeter

The detectors of the cell of the MSD-based polarimeter include two parts – the first for the measurement of the X and Y coordinates of each pair component and the second for the measurement of the X and Y coordinates of the production vertex. The second part should be done using a two-dimensional readout MSD because with a one-dimensional readout the most useful events will have only one coordinate of the vertex. The first part of the cell could be realized with a one- or two-dimensional readout. We consider below the two-dimensional readout for the third plane only.

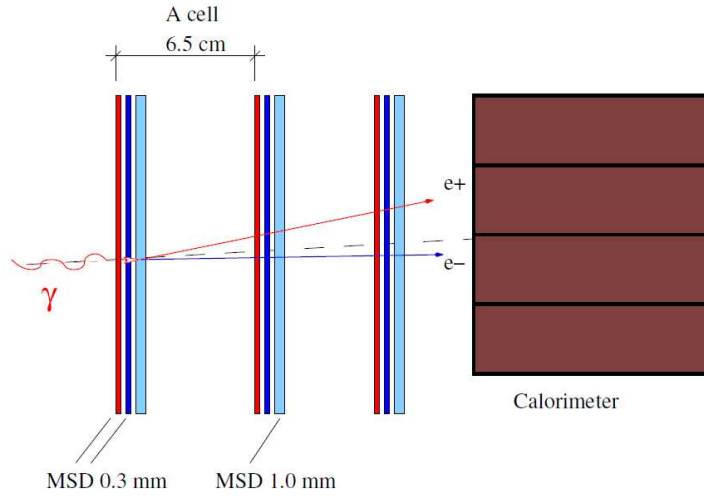


Fig. 4.— The schematic 2D view of the three cells and calorimeter of the polarimeter. The incident photon is converted into a e^+e^- pair in the 1 mm MSD.

The thickness of the silicon plate is 0.3 (1.0) mm, and the readout strip pitch is 50(100) μm for the first two (third) planes. Two first MSDs are rotated by 90° , so three planes allow determination of the coordinates in two-track events. The third plane will serve as a converter for the next cell. It provides both coordinates of the production vertex, see Fig. 4 for a three cell example. The first two MSDs also serve as veto detector(s) for the photon converted in the third MSD. A proposed 46 cell structure in a 300 cm long polarimeter leads to a cell length 6.5 cm, which allows optimal coverage of a wide range of photon energies. A calorimeter will be used for crude (10-20%) measurement of the photon energy (combined energy of the e^+e^- pair).

The configuration proposed above called for a 1 mm thickness MSD with two-sided readout strips, which is twice as large as the maximum currently available from industry. We are nevertheless expecting that such an advance in technology could be made for the current project. In any case the 1 mm converter could be replaced by two 0.5 mm converters.

8. Projected results and Conclusions

The projected results of polarization measurement are shown in Fig. 5. The photon angular resolution of the proposed system could be estimated from the MSD spatial resolution and thickness of the cell as 1 mrad for 100 MeV photon energy.

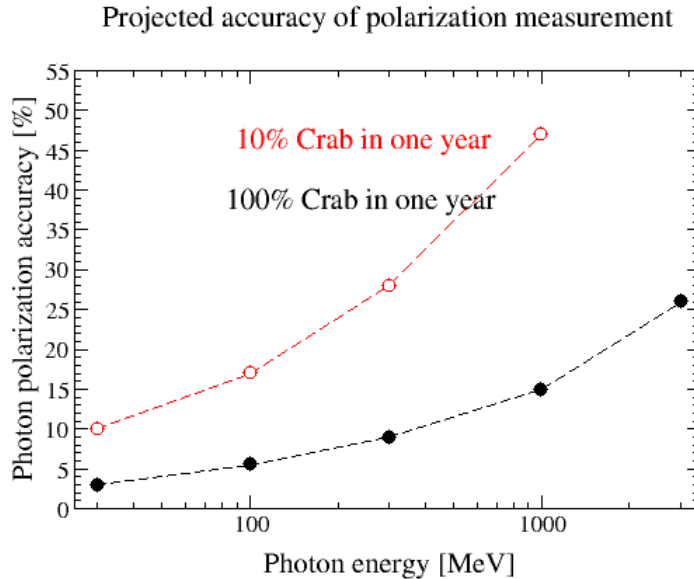


Fig. 5.— Projected accuracy of the polarization measurement with the proposed polarimeter for two levels of the incident photon intensity.

A γ ray polarimeter for astrophysics could be constructed using silicon MSD technology. Each of 46 cells will include one MSD with 2d readout of 1 mm thickness and 0.1 mm pitch and two MSDs with 1d readout of 0.3 mm thickness and 0.05 mm pitch. Using a total of 138 m² area of MSD (46 cells) and $\sim 2.8 \times 10^5$ readout channels (assuming a factor of 10 multiplexing) the polarimeter would provide a device with 9-15% photon efficiency, a 0.10 analyzing power, and a 1 mrad angular resolution. In a year-long observation, the polarization of the photons from the Crab pulsar would be measured to 6% accuracy at an energy cut of 100 MeV and $\sim 15\%$ accuracy at an energy cut of 1000 MeV.

Acknowledgements

The authors are grateful to S.D. Hunter for stimulating and fruitful discussion. We would like to acknowledge contributions by V. Nelyubin and S. Abrahamyan in the development of the MC simulation. This work is supported by NASA award NNX09AV07A and NSF CREST award HRD-1345219.

REFERENCES

- T. Young, Phil. Trans. Royal Society London, **92** 12 (1802).
- A. Michelson and E. Morley, American Journal of Science **34**, 333 (1887).
- C. N. Yang, Phys. Rev. **77**, 722 (1950); J. H. Berlin and L. Madansky, Phys. Rev. **78**, 623 (1950).
- C. Aidala, S. Bass, D. Hasch, and G. Mallot, Rev. Mod. Phys. **85**, 655 (2013), arXiv:hep-ph/1209.2803.
- P. F. Bloser *et al.*, The MEGA project: Science goals and hardware development, New Astronomy Reviews **50**, 619 (2006).
- D. Bernard and A. Delbart, Nucl. Instr. Meth. A **695**, 71 (2012); D. Bernard, Nucl. Instr. Meth. A **729**, 765 (2013), arXiv:astro-ph/1307.3892.
- F. Lei, A.J. Dean and G.L. Hills, Space Science Reviews **82**, 309 (1997).
- M.L. McConnell and J.M. Ryan, New Astronomy Reviews **48**, 215 (2004).
- M.L. McConnell and P.F. Bloser, Chinese Journal of Astronomy and Astrophysics **6**, 237 (2006).
- H. Krawczynski *et al.*, Astroparticle Physics **34**, 550 (2011).
- W. Hajdas and E. Suarez-Garcia, Polarimetry at high energies, in "Observing Photons in Space: A Guide to Experimental Space Astronomy", eds. M.C.E. Huber *et al.*, 599 (Springer, 2013).

- M. Pohl, Particle detection technology for space-borne astro-particle experiments, arXiv:physics/1409.1823.
- M. Dovciak *et al.*, MNRAS **391**, 32 (2008), arXiv:astro-ph/0809.0418.
- T. Jacobson, S. Liberati, and D. Mattingly, Annals of Physics **321**, 150 (2006), arXiv:astro-ph/0505267.
- D. Götz *et al.*, MNRAS **431**, 3550 (2013), arXiv:astro-ph/1303.4186.
- O. De Jager *et al.*, The Astrophysical Journal **457**, 253 (1996).
- S. Komissarov and M. Lyutikov, MNRAS **414**, 2017 (2011).
- V. Rusov *et al.*, arXiv:astro-ph/1401.3024 (2014).
- A. Rubbia and A. Sakharov, Astropart. Phys. **29**, 20 (2008), arXiv:hep-ph/0708.2646.
- Y.-J. Guo, X.-Y. Lai, and R.-X. Xu, Chinese Physics C **38**, 055101 (2014), arXiv:astro-ph/1209.3688.
- M. Buballa *et al.*, arXiv:astro-ph/1402.6911 (2014).
- V. M. Kaspi, M. S. Roberts, and A. K. Harding, arXiv:astro-ph/0402136 (2004).
- M. McConnell *et al.*, Astro2010: The Astronomy and Astrophysics Decadal Survey (Science White Papers, no. 198) (2009).
- P. Meszaros, Rept. Prog. Phys. **69**, 2259 (2006), arXiv:astro-ph/0605208.
- K. Toma *et al.*, The Astrophysical Journal **698**, 1042 (2009).
- C. Mundell *et al.*, Nature **504**, 119 (2013).
- M. Lyutikov, V. Pariev, and R. D. Blandford, The Astrophysical Journal **597**, 998 (2003).
- J. H. Oort and T. Walraven, Bull. Astron. Inst. Neth. **12**, 285 (1956).
- E. Bowell and B. Zellner, in Proceedings of IAU Colloq. 23: Planets, Stars, and Nebulae: Studied with Photopolarimetry, edited by T. Gehrels, p. 381 (1974).
- M. C. Weisskopf *et al.*, The Astrophysical Journal **220**, L117 (1978).
- C. J. Schrijver and C. Zwaan, Solar and stellar magnetic activity (New York: Cambridge University Press) (2000).
- J. Kovac *et al.*, Nature **420**, 772 (2002), arXiv:astro-ph/0209478.
- R. M. Kulsrud and E. G. Zweibel, Rept. Prog. Phys. **71**, 046901 (2008), arXiv:astro-ph/0707.2783.

- S. R. Kelner, Soviet Journal of Nuclear Physics **10**, 349 (1970); S.R. Kelner, Yu.D. Kotov, and V.M. Logunov, Soviet Journal of Nuclear Physics **21**, 313 (1975).
- M. L. McConnell *et al.*, in AAS/Solar Physics Division Meeting 34, Bulletin of the American Astronomical Society, Vol. 35, p. 850 (2003).
- S. E. Boggs, W. Coburn, and E. Kalemci, Astrophys. J. **638**, 1129 (2006), arXiv:astro-ph/0510588.
- M. Forot, P. Laurent, F. Lebrun, and O. Limousin, Astrophys. J. **668**, 1259 (2007), arXiv:astro-ph/0708.3724.
- S. McGlynn *et al.*, Astron. Astrophys. **466**, 895 (2007), arXiv:astro-ph/0702738.
- E. Kalemci *et al.*, Astrophys. J. Suppl. **169**, 75 (2007), arXiv:astro-ph/0610771.
- A. Morselli *et al.*, Nuclear Physics B, Proc. Supp. **239**, 193 (2013), arXiv:astro-ph/1406.1071.
- S.D. Hunter *et al.*, Astroparticle Physics **59**, 18 (2014).
- D. Bernard *et al.*, HARPO: a TPC as a gamma-ray telescope and polarimeter, arXiv:astro-ph/1406.4830; D. Bernard, HARPO: a TPC as a high-performance γ -ray telescope and a polarimeter in the MeV-GeV energy range, Conseil Scientifique du LabEx P2IO, 17 December 2014.
- A. Abdo *et al.*, The Astrophysical Journal **708**, 1254 (2010).
- F. Meddi *et al.*, Publications of the Astronomical Society of the Pacific, Volume 124, issue 195, pp.448-453 (2012); F. Ambrosino *et al.*, Journal of the Astronomical Instrumentation, Volume 2, issue 1, id. 1350006; F. Ambrosino *et al.*, Proceedings of the SPIE, Volume 9147, id. 91478R 10 pp. (2014).
- R. Buehler *et al.*, The Astrophysical Journal **749**, 26 (2012).
- H. Olsen and L. C. Maximon, Phys. Rev. **114**, 887 (1959); L. C. Maximon and H. Olsen, Phys. Rev. **126**, 310 (1962).
- B. Wojtsekhowski, D. Tedeschi, and B. Vlahovic, Nucl. Instr. Meth. A **515**, 605 (2003).
- V. Boldyshev and Y. Peresunko, Yad. Fiz. **14**, 1027 (1971), translation in the Soviet Journal of Nuclear Physics, **14(5)**, 576 (1972).
- C. de Jager *et al.*, Eur. Phys. J. A **19**, 275 (2004); arXiv:physics/0702246.